

Stripes, spin resonance and $d_{x^2-y^2}$ -pairing symmetry in FeSe-based layered superconductors

Tanmoy Das, and A. V. Balatsky

Theoretical Division, Los Alamos National Laboratory, Los Alamos, NM-87545, USA

(Dated: September 11, 2022)

We calculate RPA-BCS based spin resonance spectra of newly discovered iron-selenide superconductor using two orbitals tight-binding model. The slightly squarish electron pockets at $(\pi, 0)/(0, \pi)$ -momenta produce leading inter-pocket nesting instability at incommensurate vector $q \sim (\pi, 0.5\pi)$ in the normal state static susceptibility, pinning a strong stripe-like spin-density wave (SDW) or antiferromagnetic (AFM) order at some critical value of U . The same nesting also induces $d_{x^2-y^2}$ -pairing. The superconducting (SC) gap is nodeless and isotropic on the FSs as they are concentric to the four-fold symmetry point of the d -wave gap maxima, in agreement with various measurements. This induces an slightly incommensurate spin resonance with 'hour-glass'-like dispersion feature, in close agreement with neutron data of chalcogenides. We also calculate temperature dependence of the SC gap solving BCS gap equations and find that the spin resonance follows the same temperature evolution of $\Delta(T)$ both in energy and intensity, suggesting that an itinerant weak or intermediate pair coupling theory is relevant in this system.

PACS numbers: 74.70.-b, 74.20.Rp, 74.20.Pq, 74.20.-z

The newly discovered high-temperature superconductor in iron-selenide (FeSe-) based compounds[1], not only increase the number of unconventional SC family, but bears on several unique magnetic and superconducting properties coming from its unusual Fermi surface properties. Both ARPES[2–4] and followed by first principle calculations[5], have demonstrated that the FS is consist of two electron pockets at $(\pi, 0)$ and its equivalent points. Specific heat[6], and ARPES[2–4] studies find that these FSs are nodeless and isotropic. Evidences are mounting from NMR,[7], Raman,[8], μ SR[9], optical[10] and other experiments[11], and supported by LDA calculations[5] that these materials possess magnetic order ground state which coexists with superconductivity.

In cuprates, the FS is a hole-like centering (π, π) point and the nesting between inter FS is strongest along $Q = (\pi, \pi)$ which is responsible for SDW, $d_{x^2-y^2}$ -wave pairing and a spin resonance peak at Q with 'hour-glass' dispersion in the SC state.[12] In Ce-based heavy fermion, the hole pockets at (π, π) lead to (π, π, π) -resonance with $d_{x^2-y^2}$ -wave symmetry.[13] In iron-pnictide[14] and iron chalcogenides,[15–18] the FS has two hole-pockets at Γ and two electron-pockets at (π, π) and the leading nesting between the hole and electron pockets constitute $(\pi, 0)$ -SDW, s^\pm -pairing with (π, π) -spin resonance with a 'hour-glass' dispersion (only observed in chalcogenides). In KFeAs only one hole pocket is present at Γ and is predicted to have d -wave pairing.[19] In iron-selenide only one (or two concentric) electron-pocket(s) appeared at $(\pi, 0)$. [2–5] The role of FS topology and the interplay between electron and hole pockets and exact shape of neutron scattering intensity as a consequence of change in FS shape changes across these compounds remains a major question in the field. In this paper we investigate the unusually located electron pockets in iron-

selenide superconductors and their role in magnetic susceptibility that we find to have significant stripe like pattern; we also find that thus found spin susceptibility leads to $d_{x^2-y^2}$ -wave pairing and a spin resonance peak at Q with 'hour-glass' dispersion in the SC state.

We use an effective two band model consisting of strongly hybridized t_{2g} orbitals,[20] in tight-binding parametrization of the first principle LDA dispersion.[5] We find that the strong instability in the static susceptibility is evolved around an incommensurate vector $q = (\pi, 0.5\pi)$ at some critical value of U leading to stripe like SDW or AFM order in these systems, in agreement with experiments.[7–11] Unlike the stripe order in cuprates or other iron based superconductors, here the stripe SDW order have the same q -modulation at which a $d_{x^2-y^2}$ -pairing symmetry will posses sign change at the hot-spots.

We show that a magnetic resonance is possible at an slightly incommensurate vector in the case of $d_{x^2-y^2}$ for the relevant FS shape. Focusing mainly at one doping of $\text{Ti}_{0.63}\text{K}_{0.37}\text{Fe}_{1.78}\text{Se}_2$, and at the experimental SC gap value of 8.5meV,[3] we predict the resonance peak to be present in the range of 12.4meV at $Q = 0.78(\pi, \pi)$. The resonance profile also yields a 'hour-glass' dispersion and 45° rotation of the resonance profile, in close agreement with observations in chalcogenides[16, 17] and cuprates[12] Both the resonance energy and its intensity scales linearly with SC gap amplitude Δ and the T -dependence of the resonance energy and its intensity follows nicely with BCS form of $\Delta(T)$, vanishing at T_c . [14, 18]

Tight-binding formalism: First principle calculations show that the main contribution to the density of states (DOS) near the Fermi level comes from t_{2g} -orbitals of Fe $3d$ states which disperse only weakly in the

z -direction.[5] Similar to pnictide[20, 21], the role of the d_{xy} orbit can be approximated by a next near neighbor hybridization between d_{xz} , d_{zy} orbitals, and we consider a two-dimensional square lattice with two degenerate d_{xz} , d_{zy} orbitals per site. Based on these observations, our model Hamiltonian[20] is

$$H_0 = \sum_{\mathbf{k}, \sigma} \psi_{\mathbf{k}, \sigma}^\dagger [\xi_{\mathbf{k}}^+ \mathbf{1} + \xi_{\mathbf{k}}^- \tau_3 + \xi_{\mathbf{k}}^{xy} \tau_1] \psi_{\mathbf{k}, \sigma}, \quad (1)$$

where σ is the spin index, τ_s are Pauli matrices and $\psi_{\mathbf{k}, \sigma}^\dagger = [d_{xz\sigma}^\dagger, d_{yz\sigma}^\dagger]$ is the two component field operator. We consider up to third nearest-neighbor hopping for the present case as depicted in Fig. 1(b) which gives $\xi_{\mathbf{k}}^\pm = -(t_x^1 \pm t_y^1)(c_x \pm c_y) - 2(t_{xx} \pm t_{yy})c_x c_y - (t_x^2 \pm t_y^2)(c_{2x} \pm c_{2y}) - \mu^\pm$ and $\xi_{\mathbf{k}}^{xy} = -4t_{xy}s_x s_y$. Here $c/s_{i\alpha} = \cos/\sin(ik_\alpha a)$ for $\alpha = x, y$. $\mu^+ = \mu$ and $\mu^- = 0$.

Hamiltonian in Eq. 1 can be diagonalized straightforwardly obtaining the eigenstates $E_{0\mathbf{k}}^\pm = \xi_{\mathbf{k}}^\pm \pm \xi_{\mathbf{k}}^0$, where $\xi_{\mathbf{k}}^0 = \sqrt{(\xi_{\mathbf{k}}^-)^2 + (\xi_{\mathbf{k}}^{xy})^2}$. [20] The tight-binding parameters are obtained after fitting the dispersion to the LDA calculations,[5] Fig. 1(c): $(t_x^1, t_y^1, t_{xx}, t_{yy}, t_x^2, t_y^2, t_{xy}) = (-0.12, -0.108, -0.12, -0.12, 0.048, 0.108, 0.06)\text{eV}$ and $\mu = -0.36\text{eV}$. To obtain the experimental FS, we use rigid band shift to $\mu = -0.56\text{eV}$ and get two concentric squarish electron pockets centering $(\pi, 0)$, in good agreement with ARPES[3] shown in color plot in Fig. 1(d).

As shown below, for such FS nesting along (π, π) is most pronounced leading to a $d_{x^2-y^2}$ -pairing symmetry according to conventional views. We include SC gap with same amplitude on each band to obtain the SC quasiparticle dispersion as $E_{\mathbf{k}}^\pm = \sqrt{(E_{0\mathbf{k}}^\pm)^2 + \Delta_{\mathbf{k}}^2}$ where $\Delta_{\mathbf{k}} = \Delta_0(\cos k_x a - \cos k_y a)/2$, for the $d_{x^2-y^2}$ -gap. Δ_0 is taken from ARPES to be of 8.5meV , [3] for both eigenstates throughout this paper, except for Fig. 1(e) where an artificially large value of Δ_0 is chosen to explicate the behavior of unconventional gap opening on the DOS. In spite of the presence of nodes in the underlying gap symmetry, the dispersion at all momenta and the resulting DOS exhibit nodeless behavior in Fig. 1(e) as the FS pieces in these compounds are small in size and reside centering at the four-fold symmetric momenta of the gap maxima, similar to pnictide but unlike in cuprate. The nodeless and isotropic gap is observed in ARPES[2–4] and specific heat measurements[6].

Static susceptibility: We now proceed to the spin-susceptibility calculation of our model Hamiltonian in the SC state. The calculation of BCS susceptibility for a multiband system including matrix-element effects of all the orbitals is standard and can be found for example in Refs. 20, 21, 23. We consider the electron-electron correlation on the same Fe atom within RPA formalism.[21] The terms in the RPA interaction vertex U_s that are included in the present calculation are intraorbital interaction U , an interorbital interaction V , Hund's rule cou-

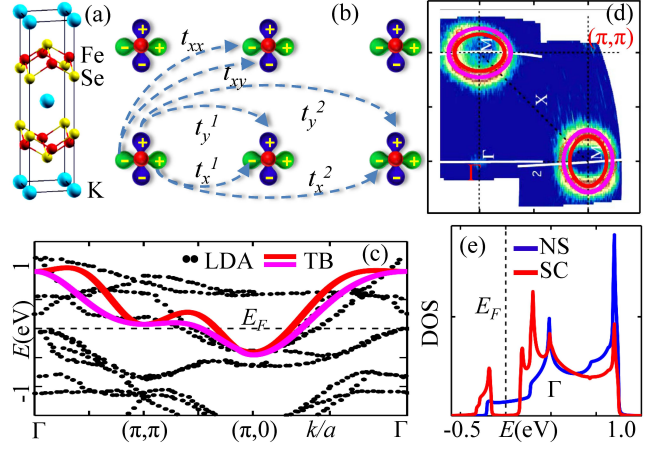


FIG. 1: (Color online) (a) Unit cell of KFe_2Se_2 -layered compound. (b) $x-y$ plane of the unit cell with Fe $3d_{xz}$ and $3d_{yz}$ orbitals is shown. The arrows depicts various hoppings considered in the present calculation. (c) The resulting two bands are plotted along high-symmetry momenta direction and compared with LDA calculation (black dots). [5] We mainly concentrate on fitting the low-energy part of the band to get the FS shape and their orbital characters in agreement with ARPES. (d) Computed electron pocket FSs overlaid on ARPES data[3]. (e) Normal state (NS) DOS is compared with its SC state result. An artificially large value of SC gap= 100meV is chosen to highlight the nodeless and isotropic nature of gap opening at E_F , despite d -wave pairing.

pling $J > 0$, and the pair hopping strength J' . In analogy to crystal and orbital symmetry of FeAs-compounds, we take $V = U - 5J/4$, $J = U/4$ and $J' = J$. [23]

Due to the specific nature of the FS shown in Fig. 1(d), the interpocket nesting is the dominant and incommensurate centering at $q = (\pi, \pi)$, see static bare susceptibility $\chi'_0(q)$ in Fig. 2(a). [22] An additional nesting occurs centered at $q = 0$ due to intrapocket nesting of the semi-squarish portion of the FSs. Note that $q = 0$ nesting is subject to the accuracy of the band structure calculation and its intensity will diminish when the FSs tend towards circular in shape with doping or for different materials. While the shape of $\chi'_0(q)$ is governed by the shape of the FS, the corresponding intensity is related to the Fermi velocity of the corresponding ‘hot-spots’. [24] Each of the $\chi'_0(q)$ pattern is split into two due to the splitting of the electron pockets into two concentric ones for our choice band parameters and chemical potential.

Within RPA, at different critical values of the interaction strengths, one or the other piece of $\chi'(q)$ will dominate, leading to SDW order phase, see Fig. 2(b-e). To clarify that, we study the evolution of the RPA susceptibility at different values of U , keeping the other interactions same with respect to the value of U (following the expressions given above). For a broad range U studied in this case, the incommensurate peak around $q = (\pi, \pi)$ is the winner, suggesting that a stripe like AFM order

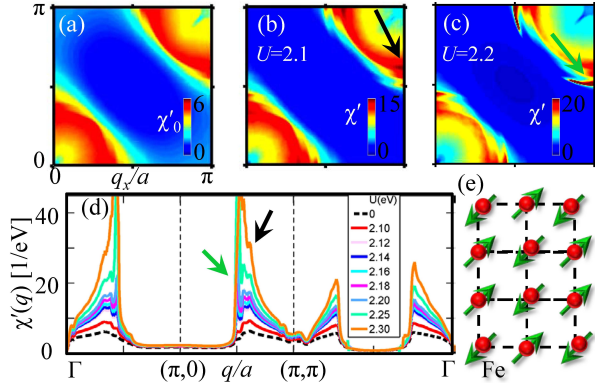


FIG. 2: (Color online) Bare static $\chi'_0(q) = \sum_{ijkl} \chi'_{0,ijkl}(q, \omega = 0)$ (i, j, k, l are orbital indices[22]) is shown in (a) and its RPA part, $\chi'(q)$, for two representative values of U are shown in (b) and (c). (d) The evolution of same $\chi'(q)$ for different values of U is drawn along the high-symmetry lines. The black and green arrows separate the peaks in $\chi'(q)$ coming from the inner and outer FS pockets (see text). (e) Schematic top view of the FeSe layer with the Fe spins in the stripe AFM order expected in our calculation are shown by the arrows.

will be present in this class of materials. These observations are consistent with LDA calculations[5] as well as with number of experiments.[7–11] In the small range of U , the inner electron pocket gains more intensity (as in the case of χ_0 , indicated by black arrows), while the outer one is comparatively small (green arrows). Interestingly, when $U > 2.2$ eV, the situation is dramatically reversed and the outer nesting develops remarkable instability properties at both around $q = (\pi, \pi)$ and $q = 0$, although the former is always dominant in the range of U studied here. With careful observation, one can find that the strong intensity in the RPA level is shifted toward $q = (\pi, 0.5\pi)/(0.5\pi, \pi)$. This specific incommensurate vector is responsible for the possible 45° rotation of the dynamical magnetic resonance spectra below the resonance energy at some critical value of U as calculated below, which is remarkably similar to the case of cuprate.

The small $q = (0, 0.46\pi)/(0.46\pi, 0)$ nesting which we find to be considerably large for our choice of parameters is close to the $q = 0$ ferromagnetic (FM) instability or may induce some form of charge-density wave (CDW) with finite q modulation. Note that the induction of CDW through SDW due to multiple nesting is an emergent phenomena predicted in heavy-fermion[25], pnictide[26] and in cuprates[24]. Scanning tunneling microscopy (STM) may be able to detect it.

Superconductivity: Unlike the $(\pi, 0)$ stripe CDW order in cuprates or $(\pi, 0)$ –stripe SDW order in pnictide, here the $q = (\pi, 0.5\pi)/(0.5\pi, \pi)$ –stripe SDW order will facilitate $d_{x^2-y^2}$ –pairing symmetry. This is due to the fact the $q = (\pi, 0.5\pi)/(0.5\pi, \pi)$ –nesting comes from the inter-electron pockets at which the $d_{x^2-y^2}$ –pairing order possess change in sign of the gap, which is the criterion

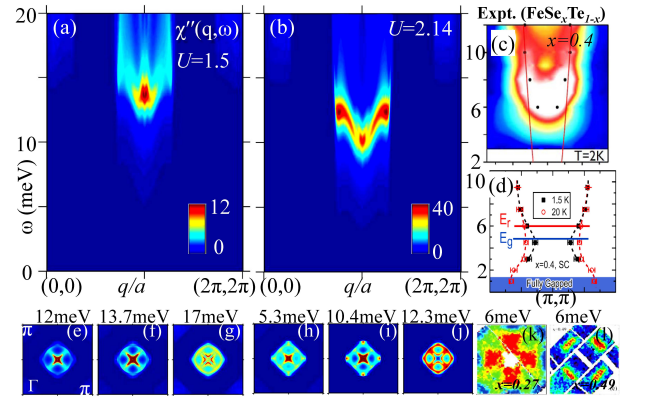


FIG. 3: (Color online) Computed BCS-RPA $\chi''(q, \omega)$ for $U = 1.5$ eV and $U = 2.14$ eV are shown in (a) and (b). The constant energy spectra at three representative energies in the lower panel of the corresponding spectra. The right-hand column shows the neutron data of $\text{FeTe}_{1-x}\text{Se}_x$, demonstrating the observations of upward dispersion[15] in (c) ‘hour-glass’ pattern[16] in (d), and 45° rotation of the spectra[17] in (k-l) in this compound.

for the spin resonance to occur as calculated below. Although, $q = (0, 0.46\pi)/(0.46\pi, 0)$ instability will provide pair-breaking contributions to the $d_{x^2-y^2}$ –symmetry.

Based on these findings, we proceed to study the evolution of the spin resonance spectra in the SC state, i.e., $\chi''(\mathbf{q}, \omega)$ (RPA-BCS) which is directly measured by Neutron scattering experiment. In the SC state, $\chi'_0(\mathbf{q}, \omega)$ is strongly enhanced for $\omega < 2\Delta$ due to turning on of the pair-scattering terms in it. This reduces the critical value of the interaction U to satisfy the RPA denominator to be positive at $U\chi'_0(\mathbf{q}, \omega) \leq 1$. We show the resonance spectra for $U = 1.5$ eV in Fig. 3(a) and $U = 2.14$ eV in Fig. 3(b) which obtain a commensurate and an incommensurate resonance respectively in addition to their characteristic dispersion.

The dispersion of $\chi''(\mathbf{q}, \omega)$ which has one-to-one correspondence to the dispersion of $\chi'_0(\mathbf{q}, \omega)$, comes from three conditions[21, 23, 27] in addition the matrix-element effects: (1) $\omega_{res}(\mathbf{q}) = \sum_{k_F^\nu, k_F^{\nu'}} |\Delta_{\mathbf{k}_F^\nu}| + |\Delta_{\mathbf{k}_F^{\nu'}}|$, (2) $\text{sgn}(\Delta_{\mathbf{k}_F^\nu}) \neq \text{sgn}(\Delta_{\mathbf{k}_F^{\nu'}})$, and (3) $\mathbf{q} = \mathbf{k}_F^\nu + \mathbf{k}_F^{\nu'}$ where ν, ν' are the band indices. Condition (1) comes from the energy conservation of inelastic scattering of Bogoliubov quasiparticles while (2) constitutes the coherence factors of BCS susceptibility to possess non-zero value. As both FS pockets have same gap symmetries and amplitudes and particularly for FeSe systems where all the FS pockets have isotropic gaps at all \mathbf{k}_F s, conditions (1) and (2) are satisfied equally at all \mathbf{k}_F s for inter electron pocket scatterings with $d_{x^2-y^2}$ –symmetry. No intensity modulation in $\chi_0(q)$ is governed by conditions (1) and (2) and the only source of intensity variation is the interplay between the orbital matrix-element effect and condition (3), the latter is simply related to the number of degenerate

\mathbf{k}_{FS} . This means, the upward dispersion of the resonance behavior in FeSe can not be understood by tracking how the gap varies on the FS as happened in cuprates[27], but only from the FS nesting and the matrix-element in the tensor form of χ_0 and also on the interaction vertex U_s . [21]

Furthermore, unlike in cuprates where the ‘hour-glass’ dispersion extends to $\omega = 0$ due to the presence of nodal quasiparticles on the FS, in nodeless FS of FeSe-compounds the spin resonance behavior spans only within Δ to 2Δ . For $U = 1.5\text{eV}$, the maximum intensity lies at the bottom of the spectra at the commensurate vector at $\omega_{res} = 13.5\text{meV}$ with $\omega_{res}/2\Delta = 0.79$. Again, $U = 2.14\text{eV}$, the maximum intensity shifts to the top of the spectra at an incommensurate vector $q = 0.78(\pi, \pi)$ at $\omega_{res} = 12.4\text{meV}$ with $\omega_{res}/2\Delta = 0.73$, slightly larger than its average value of 0.64 found in all other unconventional superconductors.[28] The upward dispersion of the magnetic spectra is qualitatively analogous to the one observed by neutron in $\text{FeTe}_{0.6}\text{Se}_{0.4}$ superconductors[15] shown in Fig. 3(c), while pnictide superconductors show more commensurate spin resonance within the experimental resolution.[14] By including the weak-intensity of the dispersion below the (π, π) –resonance, one can draw an ‘hour-glass’ feature, also seen in chalcogenides[16] in Fig. 3(d)

The constant energy profile of the resonance spectra is more interesting and bears important physical insights. At $\omega \geq \omega_{res}$ for both values of U , the resonance profile is squarish with maximum intensity lying along the diagonal and finite intensity along the (100) direction, see Figs. 3(g) and (j). For $U = 1.5\text{eV}$, the intensity remains concentrated at (π, π) even when $\omega \leq \omega_{res}$. Interestingly, for $U = 2.14\text{eV}$ at $\omega \leq \omega_{res}$ the peak along the diagonal sharply loses intensity while the intensity peak along the bond direction remains almost same. As a result, the resonance profile is rotated by 45° as one goes down below the resonance. The 45° rotation of the resonance spectra is observed earlier in hole doped cuprates[12] and can also be seen chalcogenide compounds between two different dopings in the SC state[17] in Fig. 3(k-l).

In pnictide and chalcogenide superconductors but not in cuprates, the temperature evolution of the spin resonance follows nicely the BCS mean-field behavior of the SC gap $\Delta(T)$. [14, 18] We predict that the similar phenomenon also occurs in FeSe-superconductors. To see that we calculate the $\Delta(T)$ for multiband system solving standard BCS gap equation with phenomenological pairing strength parameters $V_{1,2} = 52, 46\text{meV}$ (neglecting interband pairing). The parameters are adjusted to obtain experimental gap of $\Delta_0 = 8.5\text{meV}$ with BCS ratio $2\Delta/k_B T_c = 6.7$, in close agreement with the experimental value of 7.[3] $\Delta(T)$ is shown in Fig 4(a) (cyan line) on top of the calculated RPA-BCS spin resonance spectra at $q = (\pi, \pi)$ with $U = 1.5\text{eV}$. The intensity at the resonance is plotted in *inset* to Fig. 4(a) in red line. Both the

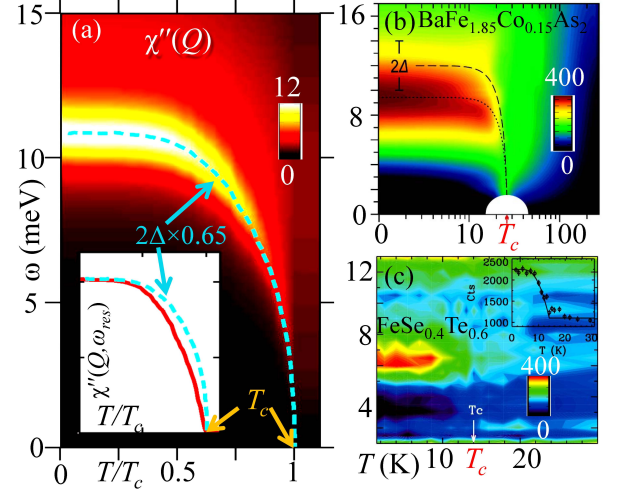


FIG. 4: (Color online) T –dependence of the spin excitation spectra at $q = (\pi, \pi)$ for $U = 1.5\text{eV}$ in (a) is compared with similar result as measured by neutron in pnictide[14] in (b) and in chalcogenides[18] in (c). *inset*: Computed value of the intensity of the resonance peak is compared with BCS $\Delta(T)$.

resonance energy and the intensity shows a remarkable one-to-one correspondence to $\Delta(T)$. The results agree well with pnictide and chalcogenide shown in Fig. 4(b,c) respectively. The present results demonstrate that the weak to moderate pair coupling theory of the spin fluctuation mechanism of superconductivity also be appropriate in FeSe-based superconductors in particular and in all iron based superconductors studied to date in general.

In summary, we have calculated the static and dynamical spin susceptibility for an effective two orbitals tight-binding model with $d_{x^2-y^2}$ –superconductivity. We find that the leading instability in the static susceptibility is evolved around an incommensurate vector $q = (\pi, 0.5\pi)$ at some critical value of U , pinning stripe like SDW or AFM order in these systems, in agreement with number of experiments.[7–11] Unlike in cuprates or other iron based superconductors, here the SDW order have the same q –vector for the $d_{x^2-y^2}$ –pairing symmetry to obtain opposite sign at the ‘hot-spot’. Our choice of parameters also predict a comparatively weak CDW modulation with $q = (0, 0.46\pi)$, similar to cuprates, heavy fermions and pnictides.[24–26] The d –wave gap yields a spin resonance behavior with ‘hour-glass’ dispersion and the 45° rotation of the resonance profile, in close agreement with observations in chalcogenides. The T –dependence of the resonance energy and its intensity follows nicely with BCS form of $\Delta(T)$, demonstrating that itinerant RPA-BCS Fermi-liquid theory will be valid in FeSe, as in other iron based superconductors.

An interesting survey can be made between all iron-based superconductors discovered to date. Both pnictide FeAs and chalcogenides SeTe possess hole pocket at Γ and electron pockets at (π, π) with s^\pm –pairing. KFeAs

compound have only hole pocket at Γ and is predicted to obtain $d_{x^2-y^2}$ -wave pairing symmetry.[19] In the present FeSe-compounds, electron pockets are formed at $(\pi, 0)$, leading to $d_{x^2-y^2}$ -pairing. Based on these observations, it is interesting to ask if the some combination of SeAs or TeAs or others may lead to two electron pockets at (π, π) and $(\pi, 0)$ or a coexistence of hole pocket at Γ and electron pocket at $(\pi, 0)$ which will induce d_{xy} -like pairing symmetry.

During the final stage of our work we became aware of preprint by T.A. Maier *et al.*[29] which also predicts the d -wave gap in FeSe based superconductors.

We are grateful to Hong Ding for useful discussion. This work was funded by US DOE, BES and LDRD and benefited from the allocation of supercomputer time at NERSC.

-
- [1] J. Guo *et al.*, Phys. Rev. B **82**, 180520(R) (2010); A. Krzton-Maziopa, *et al.*, arXiv:1012.3637; M. Fang, *et al.*, arXiv:1012.5236.
 - [2] Y. Zhang *et al.* arXiv:1012.5980.
 - [3] X.-P. Wang *et al.* arXiv:1101.4923.
 - [4] D. Mou *et al.* arXiv:1101.4556.
 - [5] C. Cao and J. Dai, arXiv:1012.5621; X.-W Yan *et al.*, arXiv:1012.5536, arXiv:1012.6015 and the references

therein.

- [6] B. Zeng *et al.* arXiv:1101.5117.
- [7] Hi. Kotegawa *et al.*, arXiv:1101.4572.
- [8] A. M. Zhang *et al.*, arXiv:1101.2168.
- [9] Z. Shermadini *et al.*, arXiv: 1101.1873.
- [10] Z. G. Chen *et al.* arXiv:1101.0572.
- [11] J. J. Ying *et al.*, arXiv:1012.5552.
- [12] P. Bourges *et al.*, Science **288**, 1234 (2000).
- [13] C. Stock *et al.*, Phys. Rev. Lett. **100**, 087001 (2008).
- [14] D. S. Inosov *et al.*, Nat. Phys. **6**, 178 (2010).
- [15] D. N. Argyriou *et al.*, Phys. Rev. B **81**, 220503(R) (2010).
- [16] S. Li *et al.*, Phys. Rev. Lett. **105**, 157002 (2010).
- [17] M. D. Lumsden *et al.*, Nat Phys. **6**, 182 (2010).
- [18] Y. Qiu *et al.*, Phys. Rev. Lett. **103**, 067008 (2009).
- [19] R. Thomale *et al.*, arXiv:1101.3593.
- [20] S. Raghu *et al.*, Phys. Rev. B **77** 220503(R) (2008).
- [21] S. Graser *et al.* New J. Phys. **11**, 025016 (2009).
- [22] We find strongest contributions from $i = j = k = l$, and the second strongest one from $i = j \neq k = l$ while the rest are negligibly small or negative.
- [23] T. A. Maier *et al.* Phys. Rev. B **79**, 134520 (2009).
- [24] R. S. Markiewicz *et al.*, Phys. Rev. B **81**, 014509 (2010); T. Das, PhD thesis, Northeastern University, Boston, MA (2009).
- [25] J.-J. Su, *et al.* arXiv:1010.0767
- [26] A. V. Balatsky *et al.* Phys. Rev. B **82**, 144522 (2010).
- [27] I. Eremin *et al.* Phys. Rev. Lett. **94**, 147001 (2005).
- [28] G. Yu *et al.* Nat. Phys. **5**, 873 (2009).
- [29] T.A. Maier *et al.* arXiv:1101.4988.